A New Method of Transient Acoustic Simulation

Zhen Wu[1,2], Milan Koch[2], Christopher Morgan[3], Enno Witfeld[2], Qiang Liu[1], Eryong Liu[1]

[1]Autoliv (Shanghai) Vehicle Safety System Technical Center, 201807 Shanghai, China
[2]Autoliv B.V. & Co. KG, Otto-Hahn-Strasse 4, 25333 Elmshorn, Germany
[3]Autoliv Auburn Hills Technical Center, 1320 Pacific Drive Auburn Hills, 48326 Michigan, USA

E-Mail: zhen.wu@autoliv.com

1 Abstract

To well understand the sound emitted by a dynamic system, transient acoustic simulation might be the best choice compared to other frequency-domain methods. However, since the human hearing frequency extends up to 20 kHz, performing a transient acoustic simulation up to this high frequency is not always possible with the traditional technologies of finite element method and boundary element method. The main reason is that the model size increases substantially with the maximum analysis frequency, which usually leads to unacceptable computational cost. This paper presents a new transient acoustic simulation method which is able to cover a full hearing frequency range from 20 Hz to 20 kHz. In particular, the method combines two types of simulations - dynamic simulation and transient acoustic simulation. In dynamic simulation, the flexible rigid-body feature of LS-DYNA® is used to compute the response of a dynamic system to external loads. With this feature, the computation effort is much reduced by representing the deformation of a finite element object by modal superposition. The surface vibrations obtained from the dynamic simulation are transferred into equivalent radiated power on each surface element, which will be further used as input for the following acoustic simulation. In transient acoustic simulation, Huygens principle is applied to simulate the emission of a sound wave from the surface of the object to any given field point. Compared to the computational cost of dynamic simulation, the cost of acoustic simulation is almost negligible. Additionally, in order to obtain more accurate results, several signal processing technologies such as resampling, DC-blocking and Gaussian window are adopted. The final result can be presented in a variety of ways – by time history of acoustic pressure, by sound map and, more important, by animation with audio. With such an auralized result, engineers do not only 'see' how a virtual dynamic system performs, but can also 'listen' to it.

2 Introduction

In general, acoustic simulation refers to a numerical procedure which aims to simulate the sound radiated by an object. A number of commercial software packages are able to perform acoustic simulation, and most of them deal with acoustic problems in the frequency domain, by using either Finite Element Method (FEM) or Boundary Element Method (BEM). Describing an acoustic problem in the frequency domain is convenient. The convenience is not only due to the ease of numerical computation, but also the simple formulations of the input and output data. For example, input the frequency response function (FRF) of a structure and output the spectrum of the sound pressure level (SPL) at a field point. However, like every coin has two faces, the frequency-domain-based acoustic simulation has its own limitations.

The major limitation comes from the transformation of the time domain into the frequency domain. As we know, both FEM and direct BEM acoustic method solve the Helmholtz equation by using Dirichlet boundary condition. In other words, if one regards the acoustic pressure at the field point as the output, then the input will be the surface vibration of the structure. Consequently, when the output is expressed in the frequency domain, the input must be expressed in the frequency domain as well. This is straightforward for load cases like steady state dynamics (SSD), because one can use the boundary condition directly from a SSD simulation. However, in most engineering cases, the surface vibration of the structure is not harmonic but highly transient. To fill the gap between the frequency domain and frequency domain, some software use discrete Fourier transformation (DFT) to convert the time-domain surface velocity to its frequency-domain counterpart. To accommodate transient signals, a DFT must either contain the entire transient signal in a long single window, or multiples uniquely sized windows, each containing a carefully chosen individual transient. Neither situation is satisfactory.

To overcome the DFT limitations, people seek to use the transient acoustic simulation. Some acoustic simulation software has this capability. The time history surface velocity is input as the boundary condition and the time history acoustic pressure is output. One could even convert this time history data to an audio file. Performing a transient acoustic simulation has its challenges. One challenge is to cover the range of human hearing frequency, which extends up to 20 kHz. Generally, the meshing criteria for acoustic simulation requires that the maximum element size should not exceed 1/6 the minimum wave length in computation. Following this criteria, the highest hearing frequency 20 kHz gives a maximum mesh size of 2.8 mm, provided the sound speed is c=340 m/s. This small mesh size usually leads to unacceptable computational cost in the automobile industry. On the other hand, the lowest hearing frequency, 20 Hz, derives large element volumes, further adding accuracy problems.

Another challenge comes from the dynamic simulation which should be performed prior to the acoustic simulation. To the best of our knowledge, most acoustic simulation software packages assume the object undergoes small deformations. In other words, rigid body motions should be avoided in the dynamic simulation. The theoretical reason behind is, both FEM and BEM acoustic methods are developed on the basis of Lagrange description of motion. In reality, however, a huge number of engineering cases contain rigid body motions. If one directly uses the surface velocity due to rigid body motion as input, then the acoustic simulation software might predict an 'unreasonable' result. We tried to use BEM method to simulate the acoustic response of a vibrating plate which is swinging about its edge. Surprisingly, the predicted sound pressure level reached 140 dB, which is almost as high as the sound pressure level generated by a fight jet flying overhead!

In this paper, we present a new simulation method for transient acoustic problems. This method contains two types of simulations: dynamic simulation and transient acoustic simulation, which will be introduced in detail in Sections 3 and 4, respectively. The dynamic simulation is performed by using the Flexible Rigid Body (FRB) feature of LS-DYNA. Compared to the traditional explicit and implicit dynamic simulation methods, the flexible-rigid-body approach reduces the degrees of freedom of a dynamic system by using a set of eigenmodes. As a result, the computational cost can be much reduced and is only proportional to the number of eigenmodes being used. This makes long time-duration calculation possible. In the transient acoustic simulation, we first discretize the outer surface of the object by a layer of triangle elements and then transfer the surface motion obtained from the dynamic simulation to the element's surface velocity. The surface velocity is further converted to the equivalent radiated power (ERP) on each element. Finally, with Huygens principle, the acoustic pressure at any given field point can be calculated by summing the sound wave radiated from each triangle element. It is worth mentioning that, our method uses a sinc-function-based filter to avoid aliasing which comes from the mismatch between the sampling frequencies of computation and audio. Moreover, the 'unreasonable' pressure offset due to rigid body motion is successfully removed by implementing another filter, called DC blocking filter. With these techniques, our method is capable of dealing with not only steady state dynamic (SSD) problems, but also other nonlinear dynamic problems which contain rigid-body motions. In Section 5, we validate our method by illustrating several examples. All results are presented in a manner of combining animation with audio, which makes 'hearing' an acoustic simulation possible. Conclusions and future work are presented in Section 6.

3 Dynamic Simulation

We might often encounter the case where an object moves in a limited space and generates sounds by colliding with its surrounding environment. Let us consider a coin which is dropped onto a stiff ground. In this case, the movement of the coin consists of two types of motions: rigid body motion and structural vibration. Compared to its rigid body motion, the structural vibration is almost negligible. However, in the acoustic simulation we must take the structural vibration into account, because it is the 'source' of the sound. That means, the vibrating structure disturbs the surrounding air and induces air pressure fluctuations. When the air pressure fluctuation propagates outward and passes through a receiver like a microphone or human hears, a sound can be recorded or perceived.

To simulate the dynamics of a dropped coin, the traditional explicit dynamic method is not efficient. In this method, the object is discretized as a finite number of elements, and the computation time step is inversely proportional to the minimum element size. When the object has a small dimension and needs a lot of fine elements to describe its geometry details, the corresponding computation time step usually drops to tens or hundreds of nanoseconds. This makes a long time-duration simulation impractical. In contrast, another method known as multi-body dynamics (MBD) efficiently computes

rigid body simulations. The method represents the object by using its 6 degrees of freedom, hence the computational cost is much lower. The disadvantage of MBD simulation is that it cannot predict structural deformation due to external loads (e.g., the collision force). Consequently it is not suitable for acoustic simulation.

After comparing the limits and merits of the two methods mentioned above, one might ask: is there any method which is able to combine the two methods together? Fortunately, the feature of flexible rigid body of LS-DYNA provides such a possibility. The basic concept of the flexible-rigid-body method is: reduce the degrees of freedom of a finite element object by only using a limited number of eigenmodes and compute its dynamics by modal superposition. In what follows, we will introduce the basic procedure of performing a flexible-rigid-body simulation.

3.1 Modal Analysis

Performing modal analysis is mandatory for a flexible-rigid-body simulation. Here it is worth noting that, although the flexible-rigid-body method supports constrained modes and attached modes, we recommend to use eigenmodes due to its clear physical meaning. In particular, each flexible-rigid body should be assigned a unique part ID and separated into an independent FE model. Elastic materials (*MAT_ELASTIC) and linear element formulations (SHELL 18 and SOLID 18) are recommended for modal analysis. Subsequently, with the two keywords *CONTROL_IMPLICIT_GENERAL and *CONTROL_IMPLICIT_EIGNVALUES, modal analysis is activated and performed for each part, namely

$$\left(\mathbf{K} - \omega^2\mathbf{M}\right)\mathbf{\Phi} = 0 . \tag{1}$$

Here $\mathbf{K}$ and $\mathbf{M}$ are the stiffness and mass matrices, $\mathbf{\Phi}$ is the modal matrix whose columns are eigenmodes, and ω are angular eigenfrequencies. The orthogonality properties of eigenmodes require that

$$\mathbf{\Phi}^{\mathrm{T}}\mathbf{M}\mathbf{\Phi} = \mathbf{I},\ \mathbf{\Phi}^{\mathrm{T}}\mathbf{K}\mathbf{\Phi} = \omega^2\mathbf{I} . \tag{2}$$

Once modal analysis is completed, all modal results, including eigenfrequencies and eignmodes, are stored in the binary database 'd3eign'. Later it will be used in the flexible-rigid-body simulation.

3.2 Flexible-Rigid-Body Simulation

In this step, all flexible-rigid-body parts must use the rigid material (*MAT_RIGID). Their part IDs should be referenced in the *PART_MODES keyword, specifying that they are not 'general' rigid bodies but are 'flexible'. Additionally, the address of the pre-calculated modal result (i.e., the 'd3eign' file) of each part should be also referenced in the *PART_MODES keyword. For each part, the equation of motion takes the form:

$$\mathbf{M}\ddot{\mathbf{u}} + \mathbf{K}\mathbf{u} = \mathbf{f} , \tag{3}$$

where $\mathbf{u}$ is the displacement, and $\mathbf{f}$ is the external loads which could be a nodal force or a contact force. Different from the traditional rigid-body simulation in LS-DYNA, the flexible-rigid-body simulation allows the users to define nodal forces and even SPC boundary conditions on a rigid body. With the properties (2), if one multiplies $\mathbf{\Phi}^{\mathrm{T}}$ on the left-hand side of equation (3), it can be rewritten as

$$\mathbf{I}\ddot{\mathbf{z}} + \omega^2\mathbf{I}\mathbf{z} = \mathbf{\Phi}^{\mathrm{T}}\mathbf{f} . \tag{4}$$

Here the vector $\mathbf{z}$ is called modal amplitude and is given by

$$\mathbf{z} = \mathbf{\Phi}^{-1}\mathbf{u},\ \ddot{\mathbf{z}} = \mathbf{\Phi}^{-1}\ddot{\mathbf{u}} . \tag{5}$$

Equation (4) is a set of second-order differential equations, which can be easily solved due to its diagonal form. Once the unknowns of $\mathbf{z}$ are solved, one can finally obtain the displacement of the part from Equation (5)

$$\mathbf{u} = \mathbf{\Phi}\mathbf{z},\ \ddot{\mathbf{u}} = \mathbf{\Phi}\ddot{\mathbf{z}} . \tag{6}$$

From the above equation, one can observe that the displacement of the object now is a sum of its eigenmodes, and each mode is weighted by a factor comes from $\mathbf{z}$. That implies the accuracy of the

calculation is only determined by the number of modes being used. Of course, we do not need a huge number of eigenmodes for calculation. The main reason is, since the maximum hearing frequency is 20 kHz, modal analysis only calculates the eigenmodes whose eigenfrequencies are less than 20 kHz. This can be defined by the parameter **RHTEND** in the *CONTROL_IMPLICIT_EIGNVALUES keyword. According to Nyquist sampling theorem, we recommend to set **RHTEND** to be 2 times as large as the highest hearing frequency, i.e., **RHTEND**=40 kHz.

3.3 Surface Motion Output

Acoustic simulation uses the surface velocity of the object as input. As a result, the final step is to extract the surface motion from the flexible-rigid-body simulation. The procedure is listed as follows. Firstly, generate a layer of triangle elements on the outer surface of the part. All triangle elements must use NULL material (*MAT_NULL). By doing this, the triangle elements are only used for data output and have no stiffness contribution to the dynamic system. Secondly, the nodes belonging to all triangle elements are defined in a node set (*SET_NODE) and output in the ASCII database 'NODOUT' (*DATABASE_NODOUT_SET). The NODOUT file contains all nodal history including node coordinates, node-displacement, velocity and acceleration.

4 Transient Acoustic Simulation

If the dynamic simulation introduced in Section 3 can be regarded as 'data generation', then the transient acoustic simulation might be regarded as 'data processing'. In other words, the transient acoustic simulation is a procedure where the data generated from the dynamic simulation is analyzed. We use HyperMath® for data processing. It is also possible to use other programming software like Scilab® and Matlab®. In what follows, we will skip the details of programming, but focus mainly on the methods and concepts behind.

4.1 Equivalent Radiated Power and Sound Propagation

Suppose da represents any surface element on the object's surface Ω. The surface element da locates at $\mathbf{x}$ and has area A, unit normal $\mathbf{n}$ and average velocity $\mathbf{v}$, as shown in Figure 1. Here the term 'element' is a convention of description of an infinitesimal surface in the context of continuum mechanics and should not be confused with the element which is used in the finite element method. If we assume the viscous shear forces of air are negligible, then the acoustic pressure, $\mathbf{p}$, on the surface element can be determined by

$$\mathbf{p} = Z(\mathbf{n} \ddot{A} \mathbf{n})\mathbf{v} = (Z\mathbf{n} \times \mathbf{v})\mathbf{n}, \tag{7}$$

where the two operators ($\ddot{A}$) and ($\cdot$) are the tensor product and dot product, respectively. Note that the pressure $\mathbf{p}$ in the above equation is a vector, whose normal is consistent with the unit normal $\mathbf{n}$, pointing outward to the field. The scalar parameter Z is the characteristic impedance of air and is given by $Z=\rho c$, where ρ is the density of air and c is the sound speed. At room temperature and under one atmosphere of pressure, Z=415 Pa·s/m.

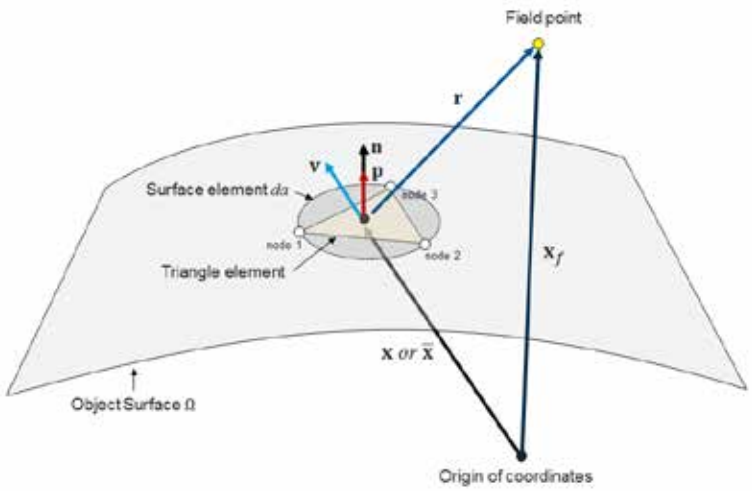

Fig.1: Illustration of surface element

The surface element *da* radiates sound power as it vibrates. The equivalent radiated power (ERP) from the surface element is given by

$$ERP = \frac{1}{2}\mathbf{p}\times\mathbf{v} = \frac{1}{2}Z\mathbf{v}\times\mathbf{v} = I\,. \tag{8}$$

Equation (8) relates the surface velocity $\mathbf{v}$ to the sound intensity I. By integrating the sound intensity I over the area of *da*, we further obtain the total sound power, that is

$$W = IA\,. \tag{9}$$

We assume the environment is anechoic. Now consider a field point f which is located at $\mathbf{x}_f$ and has a distance, $\mathbf{r}$, away from the surface element *da*. Suppose the distance r (i.e., $r=\|\mathbf{r}\|$) is large compared to the dimension of the object. In this case, it will be reasonable for us to regard the surface element *da* as a point acoustic source behaving like a monopole. It radiates sound pressure waves in the form of spherical waves. For spherical waves, the sound pressure at a far field point can be expressed as a function of the sound intensity, namely

$$p_f^2 = 2I_f Z\,. \tag{10}$$

Additionally, the inverse square law further requires that the sound intensity I_f decreases with the distance *r* squared

$$I_f = \frac{W}{4\pi r^2}\delta\,. \tag{11}$$

Here we modified the inverse square law by introducing a visibility factor, δ. For the solid object, δ takes form

$$\delta = \begin{cases} 1\,, & \mathbf{r}\times\mathbf{n} > 0 \\ 0\,, & \mathbf{r}\times\mathbf{n} <= 0 \end{cases} \tag{12}$$

The above equation assumes that there is no sound wave transmitted inside the solid object. On the other hand, when the object is sheet-like, we set δ=1. That means a sheet-like object radiates sound on its both sides. Substituting Equations (8), (9) and (11) into Equation (10), we finally obtain the sound pressure at the field point *f* due to the surface element *da*

$$p_f(t) = \sqrt{\frac{\delta A Z^2\mathbf{v}\times\mathbf{v}}{4\pi r^2}} = \frac{Z\|\mathbf{v}\|}{r}\sqrt{\frac{\delta A}{4\pi}}\,. \tag{13}$$

In Section 3, we numerically discretized the outer surface of the object by a layer of triangle elements. Noting that every triangle element has 3 nodes, we refer to the positon of each node by $\mathbf{x}_n$. Here the subscript n represents the nth node of the triangle element. The average surface velocity $\mathbf{v}$ in Equations (7) and (13) can be calculated by averaging the 3 nodes' velocities, namely

$$\mathbf{v} = \frac{1}{3}\sum_{n=1}^{3}\dot{\mathbf{x}}_n\,. \tag{14}$$

Similarly, the average center position of the triangle element is given by

$$\bar{\mathbf{x}} = \frac{1}{3}\sum_{n=1}^{3}\mathbf{x}_n\,. \tag{15}$$

Finally, the distance r in Equation (11), the area A in Equation (13) and the unit normal $\mathbf{n}$ in Equation (7) can be determined by

$$r = \|\mathbf{r}\| = \|\mathbf{x}_f - \bar{\mathbf{x}}\|, \tag{16}$$

$$A = \left\| \left(\mathbf{x}_2 - \mathbf{x}_1\right) \times \left(\mathbf{x}_3 - \mathbf{x}_1\right) \right\| / 2 , \tag{17}$$

$$\mathbf{n} = \frac{\left(\mathbf{x}_2 - \mathbf{x}_1\right) \times \left(\mathbf{x}_3 - \mathbf{x}_1\right)}{2A} . \tag{18}$$

In contrast to light, we cannot assume the propagation of sound is instantaneous. For example, consider a sound $s(t)$ generated by a speaker as shown in Figure 2. The sound can either travel straightly to the microphone (path 1), or travel by a longer distance due to the rigid reflector (path 2). As a result, the sound received by the microphone becomes

$$s_{total}(t) = s(t) + s(t - t_d) . \tag{19}$$

This phenomenon is known as echo and the time t_d is called delay. Human hear is able to detect a delay of 20 μs. In our case, the field point has a distance r away from the triangle element, which gives the delay

$$t_d = \frac{r}{c} . \tag{20}$$

Huygens principle states that the behavior of a wave front can be modeled by treating every point on the wave front as the origin of an independent monopole, and the resulting field response is the sum of the response of each monopole. Following this, we accordingly treat the object's outer surface as a wave front and each triangle element on that surface as an independent monopole. The total sound pressure at the field point f at time t can be calculated by summing the sound pressure generated by each triangle element, that is

$$P_f(t) = \sum_{[j]} p_f^{[j]}\left(t - t_d^{[j]}\right), \tag{21}$$

where the pressure in Equation (13) and the delay in Equation (20) are modified by adding a superscript with brackets, [j], indicating the element ID of the triangle element.

With the method introduced above, we now are able to compute the sound pressure at any field point from the surface motion obtained from the dynamic simulation. However, if one directly uses the raw data (i.e., the NODOUT file) as the input, usually it will cause undesired effects. For example, a sound wave which has a significant aliasing problems. To eliminate these effects, two important filters and one numerical window need to be implemented. We will introduce them in the next subsection.

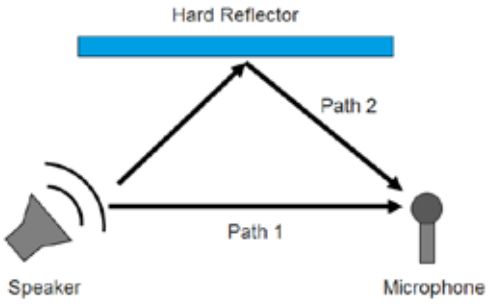

Fig.2: Example of echo and delay

4.2 Numerical Filters and Gaussian Window

Generally the dynamic simulation uses a computation time step which is much smaller than the inverse of the highest hearing frequency. For example, in our examples which will be presented in Section 5, we use a computation time-step between 10^{-5} and 10^{-6}, resulting in a sampling frequency between 100 kHz and 1000 kHz. This frequency is much higher than the highest hearing frequency, 20 kHz. However, for acoustic simulations, calculating the frequency components beyond 20 kHz are

not necessary. If the raw data in the NODOUT file is down-sampled directly from 1000 kHz to 20 kHz, the higher frequency components will cause aliasing problems, that is, the higher frequency components are overlaid and mixed together.

To avoid the aliasing problems, a low-pass filter is applied to the quantities in Equations (14) – (18). In particular, this low-pass filter is built from a combination of sinc function and Hamming window, namely

$$K_i = \mathrm{sinc}(i\Delta t)\times \mathrm{Hamming}\left(\frac{i}{5 f_{\max}\Delta t}\right), \tag{22}$$

where

$$\mathrm{sinc}(t) = \frac{\sin(2\pi f_{\max} t)}{\pi t}, \tag{23}$$

$$\mathrm{Hamming}(s) = \begin{cases} 0.54 + 0.46\cos(\pi s), & |s| \le 1 \\ 0, & |s| > 1 \end{cases}. \tag{24}$$

Here i presents the ith samples of the data, Δt is the computation time step, and f_{max} is the audio sampling frequency and is set to be 2 times as large as the highest hearing frequency, f_{max}=40 kHz.

Besides the highest frequency, the existence of the lowest hearing frequency, f_{min}=20 Hz, should also be aware. Consider, for example, an object moving at a constant velocity. Equation (7) implies that this constant velocity will generate a large, constant pressure in front of the object, which will further leads to an undesired pressure 'offset'. This 'offset' in pressure also happens in a slow-moving object such as a swinging pendulum. To remove these low frequency components, we implement a high-pass filer called DC-blocking filer. It works by first differentiating a signal and then re-integrating it again. By using Z-transformation, it can be described as

$$\frac{y_t}{x_t} = \frac{1 - z^{-1}}{1 - az^{-1}}, \tag{25}$$

where x_t is input data and y_t is output data. In the above equation, the parameter a has an important rule. It controls how much the lower frequency components will be attenuated and is given by

$$a = \frac{\sqrt{3} - 2\sin(\pi f_{\min})}{\sin(\pi f_{\min}) + \cos(\pi f_{\min})}. \tag{26}$$

The last important 'data processing' technique is the Gaussian window. In general, the delay t_d obtained from Equation (20) will not be a integer multiple of the computation time step Δt. Consequently, if we simply accommodate the delayed data from Equation (21) by rounding the delay t_d, the resulting audio will contain a lot 'spikes' and sound very buzzing. To avoid this, we apply a Gaussian window of two-sample width (i.e., the standard deviation is σ=1/2), which takes form

$$\mathrm{Gaussian}(s) = 0.5 + 0.5\,\mathrm{Erf}\left(\frac{s - i\Delta t}{s}\right), \tag{27}$$

where the error function (Erf) is given by

$$\mathrm{Erf}(x) = \frac{1}{\sqrt{\pi}}\int_{-x}^{x} e^{-t^2} dt. \tag{28}$$

The Gaussian window in Equation (27) separates a delayed data into two neighboring samples according to its cumulated possibility. Figure 3 shows a comparison of the two cases where one uses the Gaussian window and the other obtained by rounding.

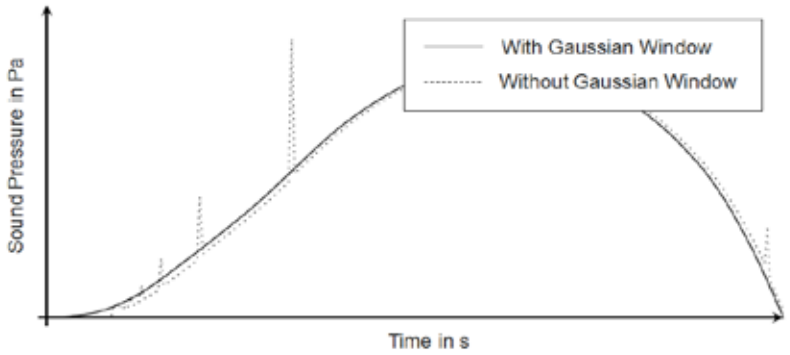

Fig.3: Comparison of the two cases with and without Gaussian window

5 Examples

In the following we validate our method by illustrating several examples. For all of the examples, the results are presented in the form of a combination of animation and audio. The animation is sampled by a rate of 25 frames per second, and the audio is sampled by using a sampling frequency of 40 kHz. Presenting auralized animations in a printed medium poses difficulty. Considering this, we present the animation by a sequence of pictures taken form the video, and present the audio by the sound pressure history or by the sound map.

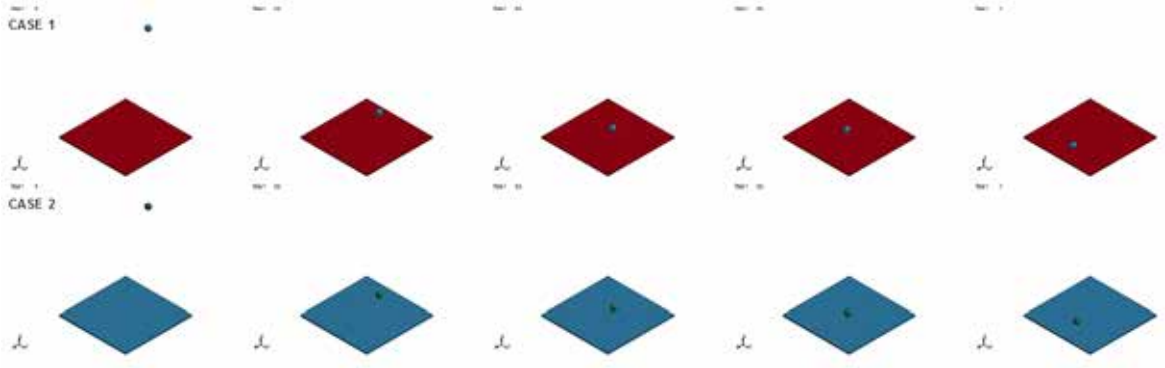

Fig.4: An aluminum ball dropping on a concrete table (CASE1) and a plastic table (CASE2)

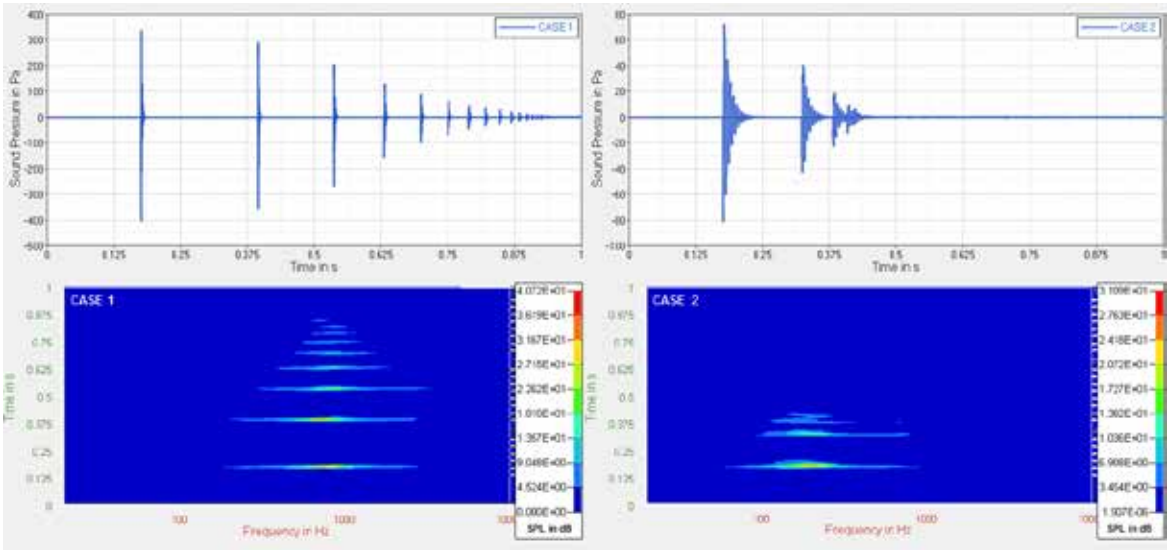

Fig.5: Comparison of the two simulation results by the sound pressure history and by the sound map

Figure 4 shows an aluminum ball dropping onto two types of tables with different material properties. One table is made of concrete and the other is made of plastic. The Young's modulus and the Poisson ratio are defined according to their real material properties. Different damping ratios are assigned for the two tables to represent the different energy dissipations of the two materials. We assume the damping is independent of frequency, so that all eigenmodes has a constant damping ratio. We use a damping ratio of 1% for the concrete table and a damping ratio of 5% is assigned for the plastic table. For both cases, the field point locates at 500 mm on the top of the table center. From Figure 5 we clearly see that, compared to the concrete table, the plastic table generates a lower frequency sound and the sound decays more quickly. If the readers have a chance to listen the resulting audio file, they will find the two simulations can not only simulate the collision sound, but also the sound when the ball is rolling on the table.

Figure 6 illustrates a vibraphone bar impacted by a stick at its center point. Vibraphone bar is a music instrument which has its fundamental frequency corresponding to one pitch frequency. The vibraphone bar used in this simulation is made of aluminum and has a fundamental frequencies of 880 Hz, which corresponds to a'' pitch according to the Helmholtz pitch notation. Please see Figure 7 for the first 4 eigenmodes. The field point is located at 300 mm on the top of the bar center. The collision force due to contact has a 'half-sin' shape, with the amplitude of 15 N and the time duration 1 ms. In reality, the vibraphone bar is supported by 4 soft rubber pins. Accordingly, we use 4 springs which have identical properties to support the finite element bar. The stiffness of the spring is adjusted so that the first eigenfrequency of the whole dynamic system is around 5 Hz. Additionally, the 4 springs have a high damping value, which is 2 times as large as its critical damping value. We can imagine, due to low stiffness of the springs, the bar will have a remarkable rigid-body motion at the beginning. This rigid body motion will cause an undesired pressure offset if the DC-blocking filter is absent. Figure 8 proofs that the DC-blocking filter can successfully remove the pressure offset and produce a more accurate result.

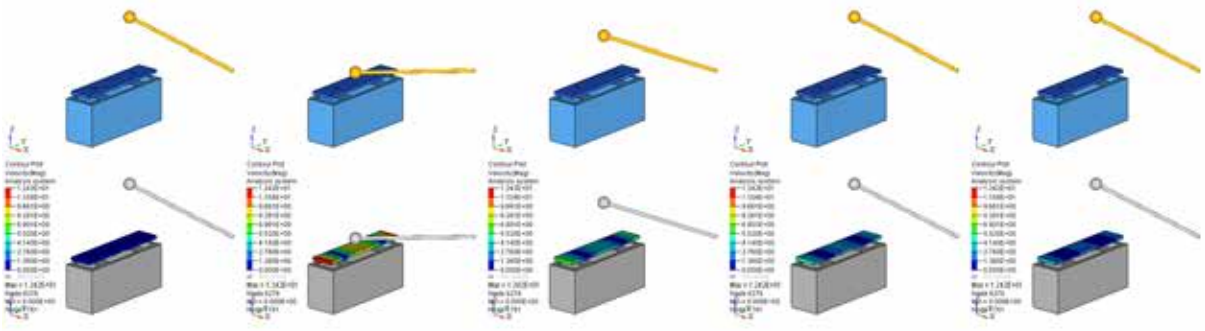

Fig.6: A vibraphone bar impacted by a stick

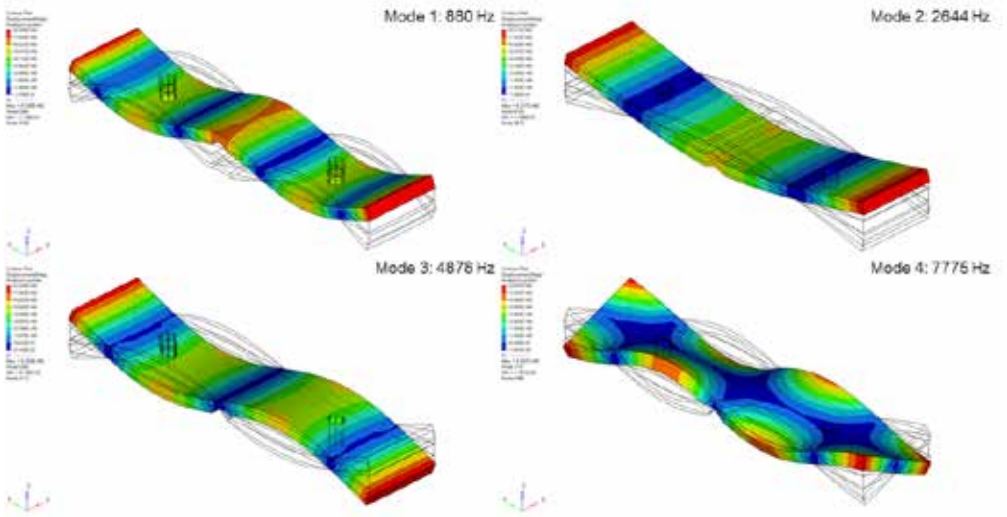

Fig.7: The first 4 eigenmodes of the vibraphone bar

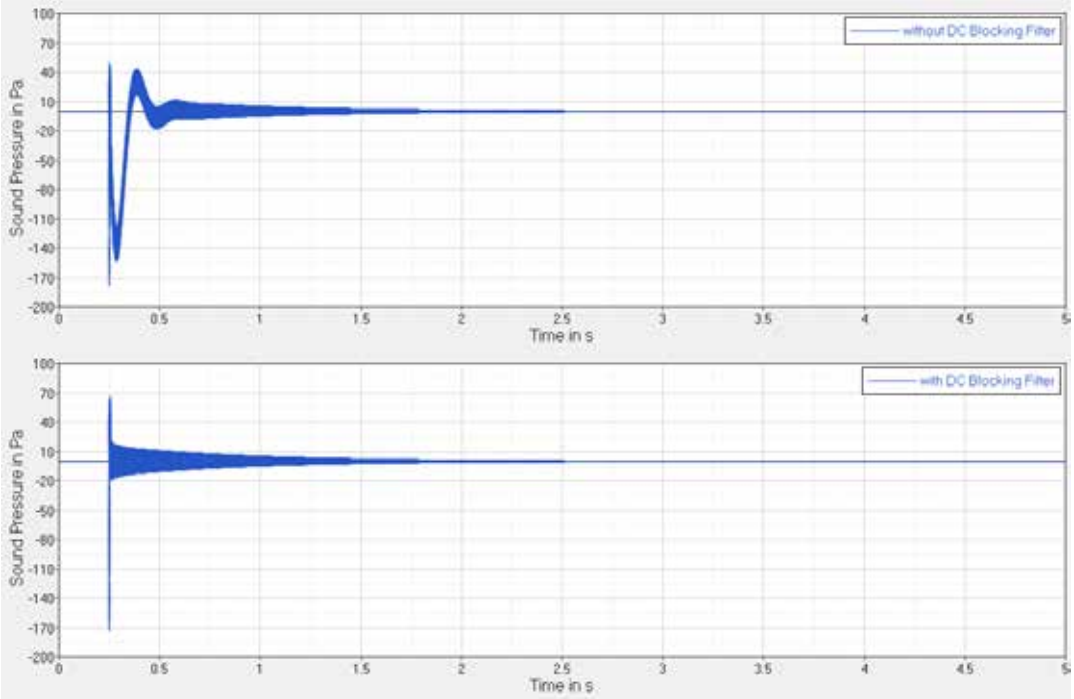

Fig.8: Comparison of the two cases with and without DC blocking filter

Figure 9 depicts a music box playing a famous song 'Jingle Bells'. The music box consists of 2 major parts: a cylinder with teeth and a comb. The cylinder is modeled as rigid and rotates at a constant speed. The comb contains 11 cantilevers, with fundamental frequencies ranging from the pitch c'' (523 Hz) to the pitch g'' (784 Hz). The positions of teeth on the cylinder are located according to the nodes of the song, and they contact with the comb as the cylinder rotates. Figure 10 shows the sound track of 'Jingle Bells' predicted by the simulation. This example shows again that, with the method developed in this paper, engineers can not only 'see' how a virtual dynamic system performs, but also 'listen' to it.

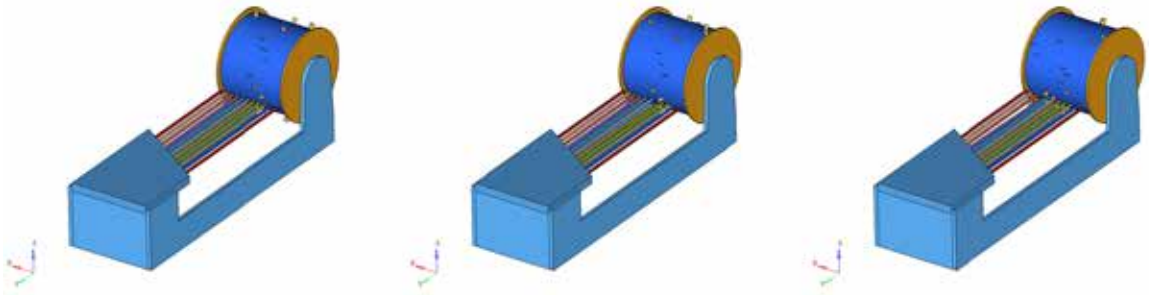

Fig.9: A music box playing a song

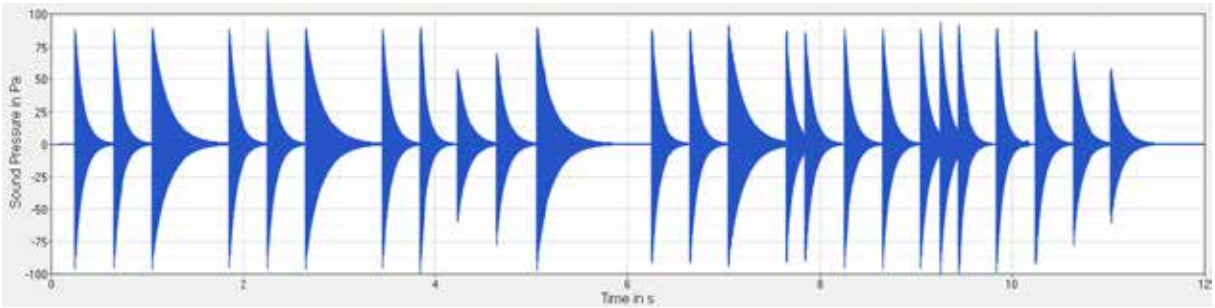

Fig.10: The sound track of 'Jingle Bells' predicted by the simulation

6 Conclusions

This paper introduced a new method for transient acoustic simulation which is able to generate auralized results. Several examples were presented, demonstrating that the developed method offers the possibility to 'listen' a virtual dynamic system.

In our method, Huygens principle is applied to estimate the sound propagation, and the effects of diffraction and scattering are ignored. As a result, one area for future work is to develop a more accurate sound radiation model. One possible way to achieve this goal might be using a pre-computed modal acoustic transfer vector (MATV). Since the flexible-rigid-body method calculates the deformation based on modal superposition, it will be reasonable to output the history of the modal amplitude $\mathbf{z}$ of each mode. On the other hand, modal acoustic transfer vector describes the relationship between eigenmodes (in the form of velocity) and the sound pressure on the object's surface. We believe that it will be very promising if the two technologies mentioned above can be included into our method.

7 References

[1] Koch M.: TRANSIENT ACOUSTIC SIMULATION WITH AURALIZATION, Master Thesis, 2017
[2] Bitzenbauer J., Schweizerhof K.: DEFORMABLE RIGID BODIES IN LS-DYNA WITH APLLICATIONS – MERITS AND LIMITS, 5th European LS-DYNA Users Conference, 2005
[3] Marker B., Benson D.: MODAL METHODS FOR TRANSIENT DYNAMIC ANALYSIS IN LS-DYNA, 7th International LS-DYNA Users Conference, 2009
[4] O'Brien J., Cook P., Essl G.: SYNTHESIZING SOUNDS FROM PHYSICALLY BASED MOTION, Proceedings of ACM SIGGRAPH 2001, 2001, 529–536
[1] O'Brien J., Shen C., Gatchalian C.: SYNTHESIZING SOUNDS FROM RIGID-BODY SIMULATIONS, ACM SIGGRAPH 2002 Symposium on Computer Animation, 2002, 175–181